JACS
JOURNAL OF THE AMERICAN CHEMICAL SOCIETY

Communication

pubs.acs.org/JACS

Crystal Structure and Superconductivity of $BaIr_2Ge_7$ and $Ba_3Ir_4Ge_{16}$ with Two-Dimensional Ba-Ge Networks

Shigeyuki Ishida,*[,†] Yousuke Yanagi,[†,‡] Kunihiko Oka,[†] Kunimitsu Kataoka,[†] Hiroshi Fujihisa,[†] Hijiri Kito,[†] Yoshiyuki Yoshida,[†] Akira Iyo,[†] Izumi Hase,[†] Yoshito Gotoh,*[,†] and Hiroshi Eisaki*[,†]

[†]National Institute of Advanced Industrial Science and Technology (AIST), Tsukuba 305-8568, Japan

[‡]IMRA Material R&D Co., Ltd., Kariya, Aichi 448-0032, Japan

Supporting Information

ABSTRACT: The Ba-Ir-Ge ternary compounds $BaIr_2Ge_7$ and $Ba_3Ir_4Ge_{16}$ exhibit superconductivity (SC) at 2.5 and 5.2 K, respectively. Detailed single-crystal structural analysis revealed that these compounds share unique quasi-two-dimensional networks composed of crown-shaped Ge rings that accommodate Ba atoms at the center, referred to as "edge-shared crown-shaped $BaGe_{16}$ polyhedra". The layered Ba-Ge network yielded a modest anisotropy of 1.3−1.4 in the upper critical field, which is in good agreement with the band structure calculations. The Ba-Ge structural unit is similar to cage structures seen in various clathrates in which the anharmonic vibration of the central atoms, the so-called "rattling" behavior, brings about strong-coupling SC. However, each Ba-Ge unit is relatively small compared to these materials, which likely excludes the possibility of unconventional SC.

Unconventional superconductivity (SC) is often associated with characteristic crystal structures. For example, unconventional SC occurs in materials possessing low-dimensional structural units, such as 2-D planes, 1-D chains, or ladder structures, which lead to enhanced spin, charge, or orbital fluctuations, resulting in non-phononic SC such as that realized in copper oxides and iron pnictides (chalcogenides).[1] Other unconventional SC candidates are materials composed of polyhedral cages, each of which accommodates one guest atom. When the cage is oversized compared to the guest atom, local low-frequency anharmonic lattice vibrations of the guest atom, the so-called "rattling" phonons, couple with the conduction electrons residing in the cages. In such cases, the electron/phonon coupling is greatly enhanced, likely leading to a higher superconducting transition temperature (T_c). The representative materials are filled skutterudites (AT_4X_{12}, A = lanthanoid, T = transition metal, X = pnictogen),[2] Ge/Si clathrates ($A_8(Ge,Si)_{46}$, A = alkaline earth),[3] and β-pyrochlore oxides (AOs_2O_6, A = alkaline atom).[4]

Recently, a series of new superconductors, $Ba_3Ir_4Ge_{16}$, $BaIr_2Ge_7$, and $Ba_3Rh_4Ge_{16}$, with T_c = 6.1, 3.2, and 6.5 K, respectively, were reported.[5] Early structural studies suggest that these compounds are composed of 2-D networks of cage units, formed by Ir(Rh)-Ge frame atoms and central Ba atoms. Based on the obtained crystal structures, the possibility of unconventional SC related to the rattling behavior has been proposed. In the present study, we performed combined crystal structural and transport studies on $BaIr_2Ge_7$ (T_c = 2.5 K) and $Ba_3Ir_4Ge_{16}$ (T_c = 5.2 K) using single-crystal samples.

Single crystals of $BaIr_2Ge_7$ and $Ba_3Ir_4Ge_{16}$ were prepared by two methods. For the self-flux method, Ba (99.9%, Furuuchi), Ir (99.9%, Western platinum), and Ge (99.999%, Furuuchi) were mixed at a molar ratio of 1:4:12 (3:4:16) for $BaIr_2Ge_7$ ($Ba_3Ir_4Ge_{16}$) and pelletized in a N_2-filled groove box. The pellets were sealed in an evacuated quartz tube, heated at 1000−1100 °C for 2 h, cooled slowly to 900 °C at a controlled rate of 2 °C/h, and then furnace-cooled to room temperature (rt). The arc-melting method was also employed. For $BaIr_2Ge_7$, Ba, Ir, and Ge were mixed at a molar ratio of 2:4:15 and melted under Ar on a water-cooled copper hearth. Single-crystal growth of $Ba_3Ir_4Ge_{16}$ by the arc-melting method was not successful.

For single-crystal X-ray structural analysis, the lattice type and lattice constants were determined using a Rigaku AFC5 diffractometer with graphite-monochromatized Mo Kα radiation (λ = 0.71069 Å). The integrated intensity data were collected by a Rigaku R-AXIS RAPID-II diffractometer, equipped with an image plate. Lorentz polarization corrections and absorption corrections were applied to all of the collected reflections. The calculations were carried out using the programs Superflip[6] and FMLSM.[7] All measurements were carried out at rt.

Magnetic susceptibility was measured using a magnetic properties measurement system (Quantum Design). The standard four-probe method was used for in-plane resistivity measurements.

We used *ab initio* band calculations to investigate the electronic structure of $Ba_3Ir_4Ge_{16}$. We used the full-potential augmented plane-wave (FLAPW) scheme, and the exchange-correlation potential was constructed within the local-density approximation (LDA), which were implemented in the KANSAI-94 and TSPACE[8] programs. The muffin-tin radii used in these calculations are 0.210a for Ba, 0.186a for Ir, and 0.167a for Ge, where a denotes the lattice constant. For the plane-wave basis functions, we used ∼2000 FLAPWs. Because this compound contains heavy Ir atoms, we included spin/orbit interaction (SOI) in the second variational approach.[9] In this scheme, we first performed the scalar-relativistic calculation and then iteratively included SOI.1

Figure 1a,c shows photographs of $BaIr_2Ge_7$ and $Ba_3Ir_4Ge_{16}$, with typical dimensions of 1.5×1.0×0.3 and 0.5×0.5×0.1 mm^3,

Received: February 6, 2014
Published: March 18, 2014

   dx.doi.org/10.1021/ja5011527 | J. Am. Chem. Soc. 2014, 136, 5245−5248

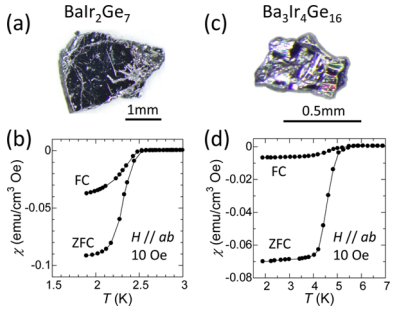

Figure 1. Top: Photographs of (a) $BaIr_2Ge_7$ and (c) $Ba_3Ir_4Ge_{16}$ single crystals. Bottom: T dependence of the magnetic susceptibility of (b) $BaIr_2Ge_7$ and (d) $Ba_3Ir_4Ge_{16}$.

Table 1. Atomic Coordinates and Equivalent Isotropic Displacement Parameters for $BaIr_2Ge_7$

atom	occ.	x	y	z	$100U_{eq}$ (Å^2)
Ba(1)	1	0.5	0.5	0.14330(10)	1.10(12)
Ba(2)	1	0.5	0	0	1.47(18)
Ba(3)	1	0	0.5	0	1.8(2)
Ir(1)	1	0	0.5	0.09794(8)	1.13(12)
Ir(2)	1	0	0.5	0.20928(8)	1.20(12)
Ir(3)	1	0.5	0	0.09823(8)	1.37(12)
Ir(4)	1	0.5	0	0.21147(8)	1.33(12)
Ge(1)	1	0	0	0.0327(2)	1.2(2)
Ge(2)	1	0.2839(9)	0	0.15290(10)	1.23(17)
Ge(3)	1	0	0.2816(6)	0.15250(10)	1.27(17)
Ge(4)	1	0.2481(6)	0.2492(6)	0.07210(10)	1.80(17)
Ge(5)	1	0.5	0.5	0.0334(2)	2.0(3)
Ge(6)	0.5	0.3580(10)	0.3650(10)	0.2221(2)	1.6(3)
Ge(7)	0.5	0.1380(10)	0.1350(10)	0.2212(2)	1.6(3)

respectively. To determine the exact crystal structure of $BaIr_2Ge_7$, a single crystal was used with dimensions of ~0.08×0.03×0.005 mm^3. In the present measurement, 12 794 reflections were detected, of which 1054 were unique, with $|F_{obs}| > 3\sigma(|F_{obs}|)$, where F_{obs} is the observed structure factor, and were employed to determine the detailed structural parameters. The observed data fulfilled a $k+l = 2n$ reflection condition, where n is an integer, based on the orthorhombic crystal system. The obtained structure belongs to orthorhombic space group *Ammm*, with lattice constants a = 6.406(4), b = 6.441(4), and c = 37.656(3) Å. We also successfully obtained anisotropic displacement parameters for all of the atoms (see Supporting Information (SI)). The final atomic coordinates and equivalent isotropic atomic displacement parameters are given in Table 1. Based on these parameters, we discuss the possibility of rattling behavior below.

Note that the space group *Pmna* was proposed previously.[5a] However, the present analysis successfully refined the anisotropic displacement parameters of all constituent atoms due to improved statistics, which were not obtained in previous studies. The refinement factor ($R = \sum|F_{obs}-F_{calc}|/\sum F_{obs}$) converged to 0.113, and the Rw ($w = 1/\sigma^2(F_{obs})$) value was 0.182. Though these values are larger than those obtained previously, in the final refinement, the condition $(\Delta/\sigma)_{max} \approx 0.001$ was satisfied, where Δ is the shift of parameters and σ is the standard uncertainty, confirming the accuracy of the present analysis. It should be also noted that structure refinement of the *Pmna* model with anisotropic displacement parameters U_{ij} could not converge in our analysis.

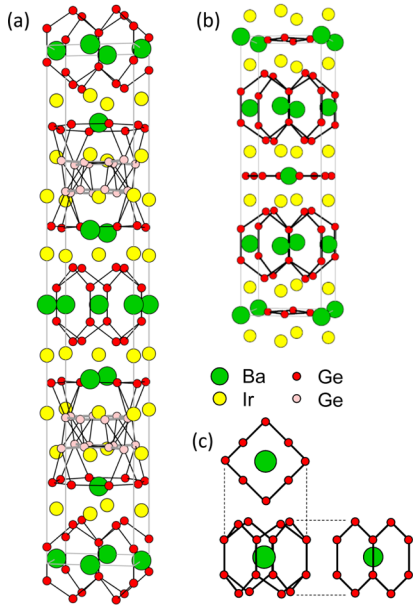

Figure 2. Crystal structures of (a) $BaIr_2Ge_7$ and (b) $Ba_3Ir_4Ge_{16}$. Green, yellow, and red correspond to the Ba, Ir, and Ge atoms, respectively. The Ge's shown in pink have 0.5 occupancy. (c) The local unit, "edge-shared crown-shaped $BaGe_{16}$ polyhedron".

The crystal structure of $BaIr_2Ge_7$ is show in Figure 2a, where Ge−Ge pairs with distances <3.0 Å are connected with each other. The longest connected pair is Ge(3)−Ge(7), at 2.892 Å. The Ge(2)−Ge(4) and Ge(3)−Ge(4) distances are 3.448(5) and 3.426(5) Å, much longer than for other connected Ge−Ge pairs. In terms of the Ge network, $BaIr_2Ge_7$ is regarded as a layered material. Here, Ba(2) and Ba(3) (they are nearly equivalent) are surrounded by 16 Ge atoms (Ge(1), Ge(4), and Ge(5)), 8 each above and below the Ba atoms, forming a crown-shaped ring unit (see Figure 2c). By sharing their edges, the rings form a 2-D array. The structural unit is thus referred to as an "edge-shared crown-shaped $BaGe_{16}$ polyhedron".

The same measurements and analysis were performed on a single crystal of $Ba_3Ir_4Ge_{16}$. This compound has a tetragonal crystal structure (Figure 2b) with space group $I4/mmm$. The crystal structure is identical to that proposed for the related compound $Ba_3Rh_4Ge_{16}$.[5a,c] The lattice constants were determined to be a = 6.5442(4) and c = 22.2833(11) Å, and the atomic displacement parameters discussed in Figure 5 were obtained (see SI). Note that $Ba_3Ir_4Ge_{16}$ also possesses layers of edge-shared crown-shaped $BaGe_{16}$ polyhedra.

Figure 1b shows the temperature (T) dependence of the magnetic susceptibility ($\chi(T)$) for $BaIr_2Ge_7$ with both zero-field-cooling and field-cooling conditions under a magnetic field of 10 Oe along the *ab* plane. The diamagnetic signal is observed below 2.5 K. A large diamagnetic signal with a shielding volume fraction of 110% at 1.8 K confirms the bulk SC in $BaIr_2Ge_7$. Figure 3a shows the T dependence of the electrical resistivity ($\rho(T)$) of $BaIr_2Ge_7$. The resistivity $\rho(T)$ decreases with decreasing T and the zero resistance is attained below 2.5 K (enlarged view shown in Figure 3b). Figure 1d shows the T dependence of the $\chi(T)$ for $Ba_3Ir_4Ge_{16}$. A large diamagnetic signal, corresponding to a 90% shielding volume fraction at 1.8 K, is observed below 5.2 K. Figure 3e shows the $\rho(T)$ of $Ba_3Ir_4Ge_{16}$. Zero resistance was observed at 5.2 K, consistent with $\chi(T)$ shown in Figure 1d.

We applied a parallel resistor model, which is a combination of the Bloch−Grüneisen term and the saturation resistivity,[10] for

dx.doi.org/10.1021/ja5011527 | J. Am. Chem. Soc. 2014, 136, 5245−5248

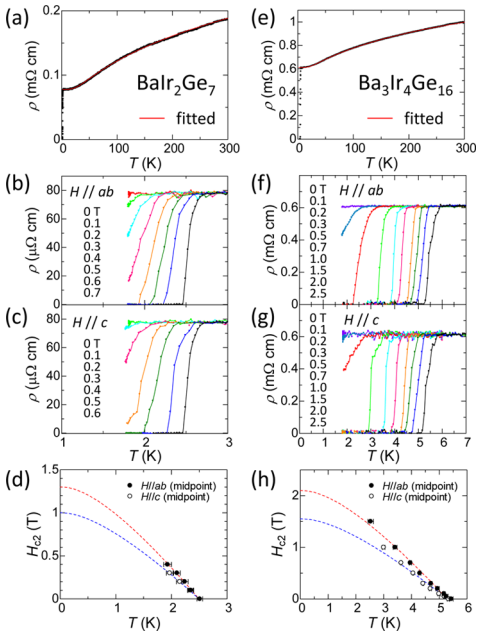

Figure 3. (a) T dependence of resistivity for $BaIr_2Ge_7$. The solid red line shows the fitting result using parallel resistor model. The resistivity $\rho(T)$ for $BaIr_2Ge_7$ below 3 K under various magnetic fields is shown for (b) $H//ab$ and (c) $H//c$. (d) T dependence of the upper critical fields of $BaIr_2Ge_7$ for $H//ab$ and $H//c$ of $BaIr_2Ge_7$. (e−h) The same set of figures for $Ba_3Ir_4Ge_{16}$.

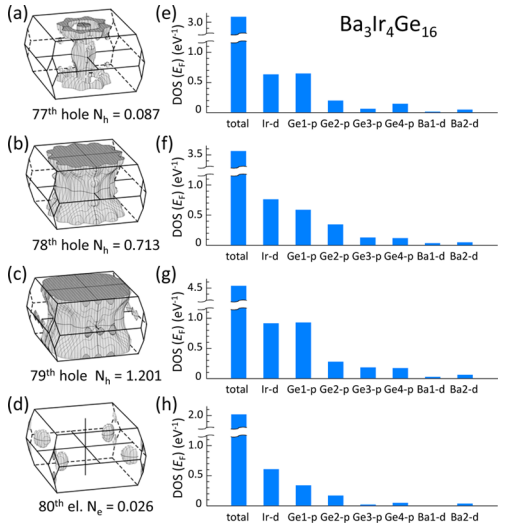

Figure 4. (a−d) Fermi surfaces of $Ba_3Ir_4Ge_{16}$. (e−h) DOS at the Fermi level for the Ir-d, Ge(1−4)-p, and Ba(1,2)-d bands.

fitting $\rho(T)$. The results are shown in Figure 3a,e (red solid lines; for the fitting procedure and obtained parameters, see SI). Although we observed a slight deviation from the fitting curve at low T, the experimental data are well fitted for overall temperatures, suggesting that the electron/phonon scattering is dominant in these compounds. Note that a deviation from T^5 dependence, namely, a smaller exponent of $\rho(T) \sim T^n$ ($n = 3-5$), can be observed in intermediately coupled and/or disordered systems.[11]

Figure 3b,c shows $\rho(T)$ for $BaIr_2Ge_7$ below 3 K under magnetic fields for $H//ab$ and $H//c$, respectively. The SC transition gradually shifts to a lower T with increasing magnetic fields, whereas the broadening of the transition width is not pronounced. This indicates that the vortex-liquid state region is narrow in $BaIr_2Ge_7$. In other words, the SC transition essentially has a 3-D nature. Figure 3d shows the T dependence of the upper critical fields, $H_{c2}(T)$, of $BaIr_2Ge_7$ for $H//ab$ and $H//c$, which is determined to be the midpoint of the transition at each magnetic field. Using the formula $H_{c2}(0) = 0.69|dH_{c2}(T)/dT|_{T=T_c}T_c$,[12] the upper critical fields at $T = 0$ are estimated as $H^{ab}_{c2}(0) = 1.3$ T for $H//ab$ and $H^{c}_{c2}(0) = 1.0$ T for $H//c$, shown as the red and blue dotted lines in Figure 3d, respectively. The anisotropy $H^{ab}_{c2}(0)/H^{c}_{c2}(0) = 1.3$, which is relatively small despite the 2-D crystal structure.

Figure 3e−h shows $\rho(T)$ at various magnetic fields for $H//ab$ and $H//c$ and the upper critical field $H_{c2}(T)$ of $Ba_3Ir_4Ge_{16}$. Here, $H^{ab}_{c2}(0)$ and $H^{c}_{c2}(0)$ are estimated to be 2.1 and 1.5 T, respectively, yielding the anisotropy $H^{ab}_{c2}(0)/H^{c}_{c2}(0) \approx 1.4$. This behavior is similar to that of $BaIr_2Ge_7$, which also indicates the 3-D nature.

The experimental results suggest that (1) $\rho(T)$ is dominated by the usual electron/phonon scattering and (2) the SC properties are rather isotropic. To see if the experimental observations can be understood within the conventional framework, we performed band structure calculations and compared them with the experimental observations.

Figure 4a−d shows the Fermi surfaces of $Ba_3Ir_4Ge_{16}$. Four bands (77−80) cross the Fermi level. Figure 4e−h depicts the total and partial density of states (DOS) for each Fermi surface. By reflecting the layered crystal structure, we see that the bands 77, 78, and 79 are basically cylindrical and open along the c-axis. While band 80 consists of small pockets, its contribution to the conductivity is less important because its DOS is much smaller than the others. Figure 4e−g demonstrates that the 2-D segments are primarily composed of the strongly hybridized Ir-d and Ge(1)-p bands. Due to the strong hybridization between these two bands, their widths are fairly broad (∼10 eV). These results support weak electronic correlation and are consistent with the low-T resistivity behavior, where the usual electron/phonon scattering plays a dominant role. At the same time, salient warping is also recognized in these bands, resulting in 3-D electronic conduction. The calculated average Fermi velocities (v_F) are 1.43×10^7 cm/s along the ab plane and 0.90×10^7 cm/s along the c axis. The anisotropy of the Fermi velocity is rather small, $v^{ab}_F/v^{c}_F \approx 1.5$, which corresponds to the anisotropy of the upper critical field, $H^{ab}_{c2}(0)/H^{c}_{c2}(0) = (v^{ab}_F/v^{c}_F)^{1/2} = 1.2$. The calculated value quantitatively agrees with the experimental one (∼1.4), indicating that the anisotropic SC of $Ba_3Ir_4Ge_{16}$ is well explained on the basis of the anisotropy of the band structure.

In the present structural analysis, we proposed $BaGe_{16}$ crowns based on connected Ge-Ge atoms. However, if we connect Ge and Ir atoms as in the previous studies, $BaIr_2Ge_7$ and $Ba_3Ir_4Ge_{16}$ are composed of a 2-D array of Ir-Ge cages. Based on the structural parameters obtained in the present study, we examine if the SC of $BaIr_2Ge_7$ and $Ba_3Ir_4Ge_{16}$ is associated with the anharmonic motion of the guest atom (Ba) within the Ir-Ge cage, which is the so-called rattling behavior. The structural parameter used as a measure of the rattling is the atomic displacement parameter (ADP). Defined as the mean-square amplitude of atomic vibration ($U_{iso} = \langle u^2 \rangle$), ADP provides information on the spatial distribution of a thermally vibrating atom. In usual materials, the regular value of $100U_{iso}$ is <2. The number is large in cage compounds, such as Ge/Si clathrates, filled skutterudites, and β-pyrochlore oxides. Particularly in the case of β-pyrochlore oxides AOs_2O_6 (A = Cs, Rb, and K), where the relationship

dx.doi.org/10.1021/ja5011527 | J. Am. Chem. Soc. 2014, 136, 5245−5248

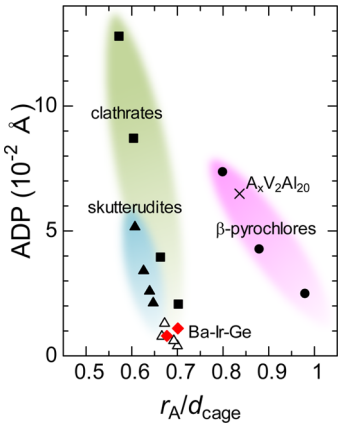

Figure 5. Relationship between r_A/d_{cage} and the atomic displacement parameter for β-pyrochlores (●), clathrates (■), skutterudites (▲, X = Sb; △, X = P), $A_xV_2Al_{20}$ (×), and Ba-Ir-Ge compounds (red diamonds).

between the SC and rattling has been experimentally established, the ADPs at rt are as large as $100U_{iso}$ = 2.48, 4.26, and 7.35 Å^2, respectively.[13] On the other hand, in $BaIr_2Ge_7$ and $Ba_3Ir_4Ge_{16}$, the ADPs of Ba atoms are quite regular ($100U_{iso} \approx 1$ Å^2) and are comparable with those of other elements, as shown in Table 1. In Figure 5, we plot the data for ADPs of various cage compounds to visualize the trends.[13] Here we employ r_A/d_{cage} as a horizontal axis, where r_A is the ionic radius of the A atom and d_{cage} is a distance from the center A atom to the nearest-neighbor cage-forming atoms (d(guest-cage)) after subtracting the radius of the cage atom (r_{cage}), i.e., $d_{cage} = d$(guest-cage) − r_{cage}. The parameter r_A/d_{cage}, which is a ratio of the size of the guest atom to the guest free space, is a key parameter for discussing the rattling energy from a structural viewpoint.[13e] For each class of cage compounds, ADP becomes larger as r_A/d_{cage} decreases (black solid symbols correspond to the so-called rattling materials). The data of $BaIr_2Ge_7$ and $Ba_3Ir_4Ge_{16}$ (red diamonds) are located around open triangle symbols, corresponding to those of P-based filled-skutterudites, which are not classified as rattling materials because their cage sizes are relatively small. Furthermore, in the case of $BaIr_2Ge_7$ and $Ba_3Ir_4Ge_{16}$, there is no clear difference in the magnitude of ADP between $BaIr_2Ge_7$, which has a smaller cage, and $Ba_3Ir_4Ge_{16}$, which has a larger cage, indicating that the rattling may not be enhanced from $BaIr_2Ge_7$ to $Ba_3Ir_4Ge_{16}$.

From the results of band structure calculations, considering the strong hybridization between the Ir-d and Ge(1)-p bands and the different character of each Ge atom, it is natural to conclude that $Ba_3Ir_4Ge_{16}$ consists of high-conductivity Ir−Ge(1) layers and low-conductivity Ba(1)−Ge(2) and Ba(2)−Ge(3,4) layers rather than the Ba(1)@[$Ge(2)_8Ge(1)_8Ir_8$] and Ba(2)@[$Ge(3)_4Ge(1)_8Ge(4)_4Ir_2$] cages proposed in previous works.[5a,b] There also exists a small but finite Ba DOS at the Fermi level, suggesting the Ba atoms have a covalent character. This is distinct from the case of β-pyrochlore oxides, where the guest atom is completely ionized and free from the cage-forming atoms, resulting in a strong rattling motion.[14] In the present case, the electron−rattler interaction, if it exists, is expected to be small.

In summary, we investigated the crystal structure of newly found Ba-Ir-Ge compounds using single crystals and proposed a correct structure model. The crystal structure can be characterized by $BaGe_6$ layers with "edge-shared crown-shaped $BaGe_{16}$ polyhedra". The detailed structural analysis, transport study, and band structure calculations likely exclude the possibility of rattling behavior having a role in the superconductivity. Instead, the novel Ba-Ge network is likely to be relevant to the emergence of superconductivity in the present Ba-Ir-Ge system.

■ ASSOCIATED CONTENT

Ⓢ Supporting Information

Atomic coordinates and atomic displacement parameters for $Ba_3Ir_4Ge_{16}$, fitting procedure for $\rho(T)$, and crystallographic data (CIF). This material is available free of charge via the Internet at http://pubs.acs.org.

■ AUTHOR INFORMATION

Corresponding Author

s.ishida@aist.go.jp; y-gotoh@aist.go.jp; h-eisaki@aist.go.jp

Notes

The authors declare no competing financial interest.

■ ACKNOWLEDGMENTS

This work was partly supported by Strategic International Collaborative Research Program (SICORP), Japan Science and Technology Agency (JST).

■ REFERENCES

(1) (a) Lee, P. A.; Nagaosa, N.; Wen, X. G. *Rev. Mod. Phys.* **2006**, *78*, 17. (b) Stewart, G. R. *Rev. Mod. Phys.* **2011**, *83*, 1589.

(2) Keppens, V.; Mandrus, D.; Sales, B. C.; Chakoumakos, B. C.; Dai, P.; Coldea, R.; Maple, M. B.; Gajewski, D. A.; Freeman, E. J.; Bennington, S. *Nature* **1998**, *395*, 876.

(3) Nolas, G. S.; Cohn, J. L.; Slack, G. A.; Schujman, S. B. *Appl. Phys. Lett.* **1998**, *73*, 178.

(4) Yonezawa, S.; Muraoka, Y.; Hiroi, Z. *J. Phys. Soc. Jpn.* **2004**, *73*, 1655.

(5) (a) Falmbigl, M.; Grytsiv, A.; Rogl, P.; Giester, G. *Intermetallics* **2013**, *36*, 61. (b) Guo, J.; Yamaura, J.; Lei, H.; Matsuishi, S.; Qi, Y.; Hosono, H. *Phys. Rev. B* **2013**, *88*, 140507(R). (c) Falmbigl, M.; Kneidinger, F.; Chen, M.; Grytsiv, A.; Michor, H.; Royanian, E.; Bauer, E.; Effenberger, H.; Podloucky, R.; Rogl, P. *Inorg. Chem.* **2013**, *52*, 931. (d) Duong Nguyen, H.; Prots, Y.; Schnelle, W.; Böhume, B.; Baitinger, M.; Paschen, S.; Grin, Y. Z. *Anorg. Allg. Chem.* **2014**, DOI: 10.1002/zaac.201300599.

(6) Palatinus, L.; Chapuis, G. *J. Appl. Crystallogr.* **2007**, *40*, 786.

(7) Kato, K. *Acta Crystallogr.* **1994**, *A50*, 351.

(8) Yanase, A. *Fortran Program for Space Group* (TSPACE) (in Japanese); Shokabo: Tokyo, 1995.

(9) Koelling, D. D.; Harmon, B. N. *J. Phys. C: Solid State Phys.* **1977**, *9*, 3107.

(10) Wiesmann, H.; Gurvitch, M.; Lutz, H.; Ghosh, A.; Schwarz, B.; Strongin, M.; Allen, P. B.; Halley, J. H. *Phys. Rev. Lett.* **1977**, *38*, 782.

(11) Gurvitch, M. *Phys. Rev. Lett.* **1986**, *56*, 647.

(12) Werthamer, N. R.; Helfand, E.; Hohenberg, P. C. *Phys. Rev.* **1966**, *147*, 295.

(13) (a) Yamaura, J.; Yonezawa, S.; Muraoka, Y.; Hiroi, Z. *J. Solid State Chem.* **2005**, *179*, 336. (b) Yamaura, J.; Hiroi, Z. *J. Phys. Soc. Jpn.* **2011**, *80*, 054601. (c) Matsuhira, K.; Sekine, C.; Wakeshima, M.; Hinatsu, Y.; Namiki, T.; Takeda, K.; Shirotani, I.; Sugawara, H.; Kikuchi, D.; Sato, H. *J. Phys. Soc. Jpn.* **2009**, *78*, 124601. (d) Sales, B. C.; Chakoumakos, B. C.; Jin, R.; Thompson, J. R.; Mandrus, D. *Phys. Rev. B* **2001**, *63*, 245113. (e) Hiroi, Z.; Onosaka, A.; Okamoto, Y.; Yamaura, J.; Harima, H. *J. Phys. Soc. Jpn.* **2012**, *81*, 124707.

(14) (a) Saniz, R.; Medvedeva, J. E.; Ye, L. H.; Shishidou, T.; Freeman, A. *J. Phys. Rev. B* **2004**, *70*, 100505(R). (b) Hiroi, Z.; Yamaura, J.; Yonezawa, S.; Harima, H. *Physica C* **2007**, *20*, 460.